Applied Surface Science 261 (2012) 722–726

Contents lists available at SciVerse ScienceDirect

Applied Surface Science

journal homepage: www.elsevier.com/locate/apsusc

An alternative approach for femtosecond laser induced black silicon in ambient air

Yuncan Ma, Hai Ren, Jinhai Si*, Xuehui Sun, Haitao Shi, Tao Chen, Feng Chen, Xun Hou

Key Laboratory for Physical Electronics and Devices of the Ministry of Education & Shaanxi Key Laboratory of Information Photonic Technique, School of Electronics and Information Engineering, Xi'an Jiaotong University, Xianning West Road 28, Xi'an 710049, China

ARTICLE INFO

Article history:
Received 16 May 2012
Received in revised form 17 July 2012
Accepted 23 August 2012
Available online 5 September 2012

Keywords:
Black silicon
Femtosecond laser
Selectively etching
Absorption
Ambient air

ABSTRACT

An alternative approach for femtosecond laser induced black silicon in ambient air is proposed, in which, black silicon is fabricated on a tellurium coated silicon substrate via femtosecond laser irradiation in ambient air, and selectively etching with hydrofluoric acid is employed to remove the incorporated oxygen. Results of energy dispersive X-ray spectroscopy analysis and absorption measurement show that oxygen is effectively eliminated via etching, and the optical absorption of the black silicon is enhanced.

1. Introduction

As one of the most popular materials in semiconductor industry, silicon has extensive applications in silicon based solar energy cells and optoelectronic detectors. However, the band gap of silicon is 1.12 eV (λ_g = 1100 nm), incident photons with wavelength longer than 1100 nm cannot be absorbed, which limits the applications of silicon in the infrared region. Reducing the reflection of silicon is an effective way to enhance its optical absorption; therefore, more and more research interests have been concentrated on this topic [1–4].

Since Mazur and co-workers firstly reported the femtosecond laser induced black silicon in SF_6 or Cl_2 [5], the near-unity below-band-gap absorption of this novel microstructure has inspired more and more researchers [6–8], and this silicon structured via femtosecond laser irradiation has potential applications in silicon based photovoltaics [9–12], photodetectors [13], terahertz emitter [14] and superhydrophobic devices [15,16]. As the incorporation of oxygen (O) species into the irradiated silicon may have influences on the material and structural characteristics of silicon, most of the current reports on the femtosecond laser induced black silicon are conducted in ambient gases [17–20] or vacuum [21,22]. Meanwhile, recent investigations suggest that the chalcogen species (sulfur, selenium, and tellurium) doped silicon prepared by pulsed laser irradiation or ion implantation also exhibits enhancement of absorption in the near-infrared region [23–26]. However, up to the date, there have not been reports on direct fabrication of black silicon with enhanced near-infrared absorption in ambient air.

In this paper, we propose an alternative approach for the black silicon produced in ambient air. The advantages of this approach include the simplification for the experimental devices and the feasibility for the post-treatment of the samples. In the experiments, chalcogen tellurium (Te) was chosen as the dopant precursor on the silicon substrates, and the reasons are below: firstly, there have been reports on the incorporation of chalcogen species such as sulfur (S) or selenium (Se) into silicon by laser irradiation [9,19,26], but reports on that of tellurium (Te) are absent; secondly, the bulk diffusivity of Te in crystal silicon (c-Si) is the smallest among the three kinds of chalcogen species [24], which would be beneficial for enhancement of the absorption of the sample which bears thermal annealing; finally, the melting point of Te is the highest among the three kinds of chalcogen species, which would be convenient to control the film thickness in the process of thermal evaporation. The black silicon was produced on a tellurium (Te) coated silicon substrate with a femtosecond laser irradiation. The irradiated sample was first annealed in ambient air and then selectively etched by hydrofluoric acid (HF) respectively. Results of energy dispersive X-ray spectroscopy (EDS) analysis show that Te and O are incorporated into silicon after irradiation and thermal annealing; when the sample is selectively etched with HF, the O species is effectively removed. Furthermore, the optical absorptance of the black silicon reaches to approximately 90% and 80% in the visible

* Corresponding author. Tel.: +86 029 82663485.
E-mail address: jinhaisi@mail.xjtu.edu.cn (J. Si).

0169-4332/$ – see front matter © 2012 Elsevier B.V. All rights reserved.
http://dx.doi.org/10.1016/j.apsusc.2012.08.087

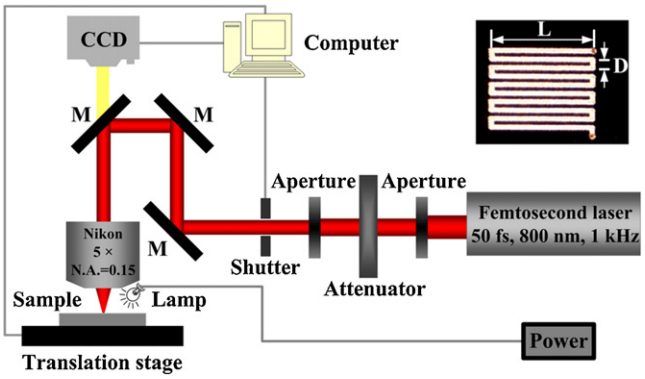

Fig. 1. Schematic illustration for the fabrication of black silicon in ambient air.

and near-infrared regions respectively, after thermal annealing the absorptance decreases to 80% and 60% respectively. What is more, the absorption of the black silicon in the visible region is enhanced and that in the near-infrared region keeps almost invariant after etching, which is important to the practical applications of the black silicon fabricated in ambient air.

2. Experimental details

An amplified Ti: sapphire femtosecond laser system (Coherent Inc., U.S.A.) was employed to provide laser pulses with 50 fs pulse duration, 800 nm wavelength, and 1 kHz repetition rate. The spatial profile of the laser beam was Gaussian. Fig. 1 shows the schematic illustration for the fabrication of black silicon in ambient air. The energy of the incident laser pulses could be continuously varied by rotating a variable neutral density filter (NDF), and the access of the laser was controlled via a mechanical shutter connected to a computer.

The n-type Si (1 1 1) wafers, with a thickness of 300 μm and a resistivity of 3000 Ωcm, were previously ultrasonic cleaned in acetone, ethanol and de-ionized water for 15 min respectively, then a thin Te film (about 500 nm) was deposited onto the silicon substrates at a rate of 2–3 nm/s via thermal evaporation in vacuum. After that the Te coated wafers were mounted on a computer controlled three-dimensional translation stage (ProScan II^{TM}) with a step resolution of 40 nm at x, y and z-axis respectively. The linearly polarized laser beam was focused onto the silicon surface by a 5× microscope objective (Nikon) with a numerical aperture (NA) of 0.15. The size of the laser spot (approximately 30 μm) was determined by measuring the diameters of the photoinduced craters via a single laser pulse (at the same average laser power and z position as used in the experiments) attacked the substrate, and the accuracy of the calculated laser fluence was guaranteed by calculating the average diameter of more than ten induced craters. The inset image in the upper right corner of Fig. 1 illustrates the scanning path of the laser beam on the substrate; in this image L is the length of the scanning lines, and D is the interval between two adjacent scanning lines. Furthermore, the scanning direction was parallel to the polarization direction of the incident laser.

A CCD camera was used to monitor the fabrication progress, and an optical fiber lamp was employed to assist the observation. After irradiation, the wafers with a structured 12 mm × 12 mm area were firstly annealed at a temperature of 775 K for 45 min in ambient air and then selectively etched with 10% HF for 10 min respectively. The morphology and chemical composition of the black silicon were characterized by scanning electronic microscopy (SEM) equipped with an energy dispersive X-ray spectroscopy (EDS) (JEOL JSM-6390A series). The reflectance (R) and transmittance (T) of the black silicon at the wavelengths ranging from 400 nm to 2500 nm were measured at an increment of 2 nm respectively via a UV-vis-NIR spectrophotometer equipped with an integrating sphere (JASCO Corp., V-570, Rev. 1.00), then the absorptance (A) was calculated by the formula: $A = 1 - R - T$.

3. Results and discussion

The black silicon was produced at the laser fluence (E) of 0.85 J/cm^2, the scanning velocity (υ) of 500 μm/s, and the scanning interval (D) of 10 μm. Fig. 2 shows the SEM images of the black silicon. As is evident from Fig. 2, the black silicon is composed of many independent spikes distributed quasi-uniformly on the substrate. The height of the spikes is about 8–10 μm, the scale of the top is about 2–3 μm, and the average space between two adjacent spikes is about 4–5 μm. Meanwhile, the surface of the spikes is mantled with many nano-particles. The formation of the spikes could be attributed to the solidification driven extrusion (SDE): the material melt under the laser irradiation, then nucleation occurred at the gas–solid interface and the frozen mantle grew inward from the surface. Because of the expansion of the liquid material, the freezing mantle placed the liquid material under pressure. When the pressure built up sufficiently, the weakest position in the mantle gave way and the liquid material was forced out, then the spikes formed [27–29]. The size of the spikes depends on the processing parameters such as the incident laser fluence, the scanning velocity, the interval between two adjacent scanning lines and the laser polarization.

Fig. 3 shows SEM images of the irradiated silicon after thermal annealing (Fig. 3(a) and (b)) and chemical etching (Fig. 3(c) and (d)). In comparison with Fig. 2(b), there is little change in morphology after thermal annealing to the resolution of the SEM (see Fig. 3(b)); meanwhile, the number of the nano-particles decreases after etching with HF (see Fig. 3(d)).

In order to measure the chemical composition of the black silicon, EDS analysis was conducted at the positions (means points A–H) marked in Figs. 2 and 3, results of which were illustrated in Fig. 4. We can see in Fig. 4 that the chemical composition of the irradiated Te coated silicon are Te, O and Si, while that of the uncoated silicon are O and Si. For the coated sample, the maximum atomic percentage of Te incorporated into the black silicon reaches 0.69%, while that of O reaches 44.84%. We employ the following two mechanisms to explain the incorporation of Te and O respectively. Firstly, when the coated silicon is irradiated by the laser pulses with a fluence far beyond the ablation threshold of silicon, the substrate is ablated due to the energy transfers to the cold lattice through electron-photon coupling, then the chalcogen Te is trapped in the plume of laser ablated material, and the redeposition is responsible for the small amount of Te that is incorporated into silicon (just as S or Se is incorporated into silicon in the work of Mazur and coworkers) [19,24]. Secondly, with the femtosecond laser irradiation, some crystal silicon (c-Si) transforms to amorphous silicon (a-Si) [30]. As we know, the atoms in amorphous silicon (a-Si) do not arrange as regularly as those in crystal silicon (c-Si), thus dangling bonds appear in the silicon lattice. These bonds would trap the O atoms in ambient environment into the interior of silicon. This is known as the laser induced trapping effect of the dangling bonds [31–33].

We can also see in Fig. 4 that the content of Te decreases while that of O increases after thermal annealing. The content of Te decreased due to the diffusion of Te in the annealing process; meanwhile, annealing was conducted in ambient air, silicon would be oxidized at the temperature of 775 K, thus the content of O increased. As we know, the incorporated O may influence the material and structural characteristics of silicon substrates; therefore, in order to remove the incorporated O species, a simple

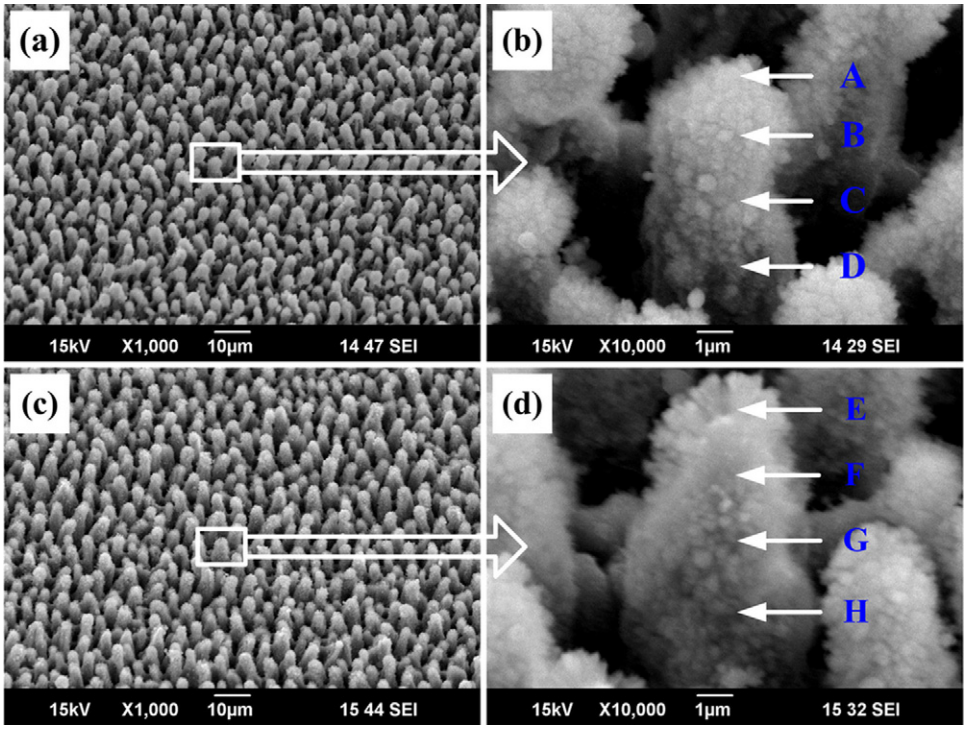

Fig. 2. SEM images of the irradiated silicon. (a) Te coated silicon; (b) detailed morphology of the zone marked in (a); (c) uncoated silicon; (d) detailed morphology of the zone marked in (c). The fabrication parameters: $E = 0.85\,J/cm^2$, $\upsilon = 500\,\mu m/s$, $L = 12\,mm$, $D = 10\,\mu m$. EDS analysis was conducted at the positions marked in (b) and (d). These images were taken at an angle of 45° from the silicon surface.

approach, selective etching with HF, was employed; and mechanism of which could be explained as the following chemical reactive formula [34,35]:

$$SiO_2(s) + 6HF(aq) \rightarrow H_2SiF_6(aq) + 2H_2O(aq)$$

Then the etched sample was ultrasonically rinsed in de-ionized water for 15 min to remove the reactants such as HF and H_2SiF_6. Results of the EDS analysis show that O was effectively eliminated, and the Te content was not decreased but rather relatively

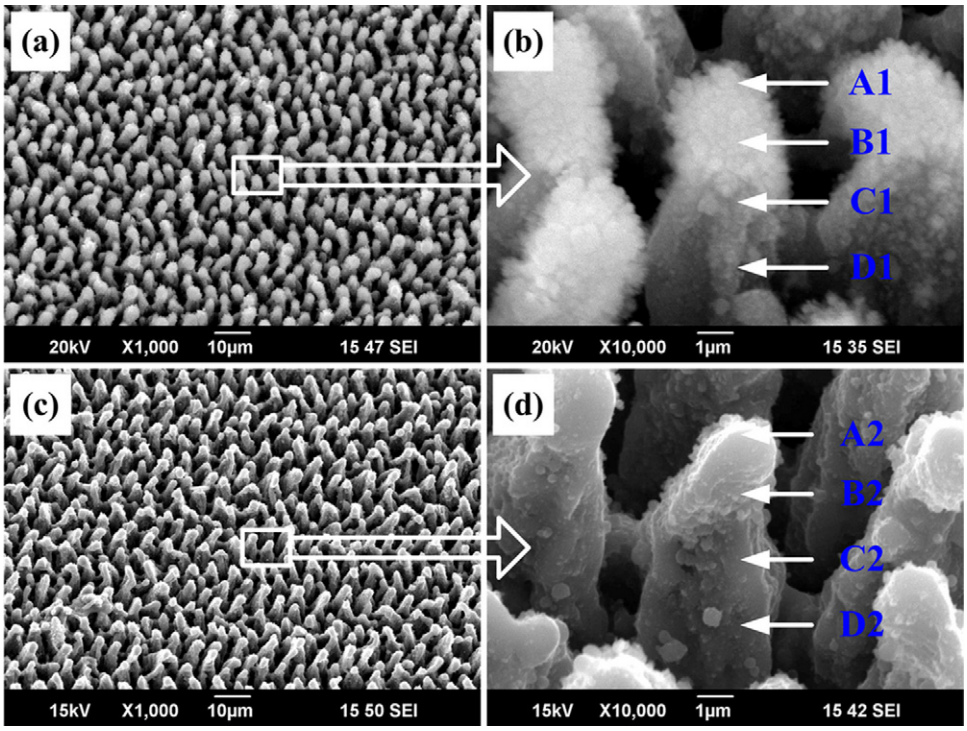

Fig. 3. SEM images of the Te coated silicon wafers with different post-treatments. (a) Annealing at a temperature of 775 K for 45 min in ambient air; (b) the detailed morphology of the zone marked in (a); (c) etching with 10% HF for 10 min; (d) the detailed morphology of the zone marked in (c). EDS analysis was conducted at the positions marked in (b) and (d). These images were taken at an angle of 45° from the silicon surface.

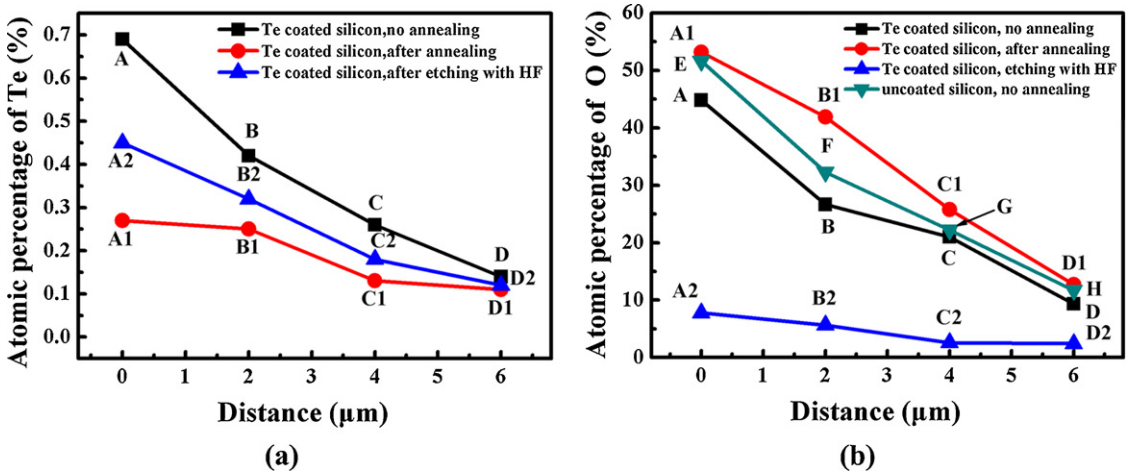

Fig. 4. Atomic percentage of (a) Te and (b) O at the positions marked in Fig. 2 and Fig. 3.

increased (the absolute number of Te atoms certainly does not increase but the concentration relative to Si increases) after etching with HF (see Fig. 4(b)), which means that the chalcogen Te has been preferentially captured in the predominant Si rather than the SiO_2 containing regions. What is more, no additional impurities were introduced; however, the influence of chemical etching on the optical property of black silicon needs to be further investigated.

We measured the optical absorptance of the irradiated Te coated silicon with different post-treatments, results of which are shown in Fig. 5. In comparison with flat silicon (see Fig. 5 curve (a)), the irradiated Te coated wafer shows enhanced absorption at the measured wavelengths ranging from 400 nm to 2500 nm. After irradiation, the absorptance of the Te coated silicon reaches to approximately 90% and 80% in the visible and near-infrared regions (see Fig. 5 curve (b)) respectively. As for the enhancement of the optical absorptance for the irradiated Te coated silicon, two mechanisms have been proposed to explain it: in the wavelength range of $\lambda < \lambda_g$, the geometry light trapping, which results from the multiple reflections of the incident light due to the formation of micrometer-sized silicon spikes, contributes to the enhancement of the absorption [9], and the parameters of the spikes (such as height, space, and subtended angle) determine the extent of the absorption enhancement in this region; in the wavelength range of $\lambda > \lambda_g$, the incorporation of intermediate band into the band gap of silicon, which decreases the absorption threshold of the material to the incident photons (this means incident photons with wavelength longer than 1100 nm could be absorbed by the material), is the main reason for the enhancement of the absorption [9,24–26], and the state density of the intermediate band determines the extent of the absorption enhancement in this region. When the sample is annealed, the state density of the intermediate band gap decreases due to the diffusion of Te to the crystalline grain boundary. Therefore, the optical absorptance in the near-infrared region decreases (see Fig. 5 curve (c)). We can also see curve (d) in Fig. 5 that the absorptance of the etched black silicon enhances slightly in the visible region and that in the near-infrared region keeps almost invariant. This could be well explained by the mechanisms depicted above. After selective etching with HF, the spikes become smoother and sharper due to the decrease in the nano-particles, the height, space and subtended angle of the spikes increases; therefore, the incident angle of the light increases and then the incident light could be effectively trapped due to the multiple reflections at the silicon–air interface; meanwhile, the incorporated Te is nearly not influenced by the selectively etching with HF, the state density of the immediate band gap changes little, thus the absorptance in the near-infrared region keeps almost invariant.

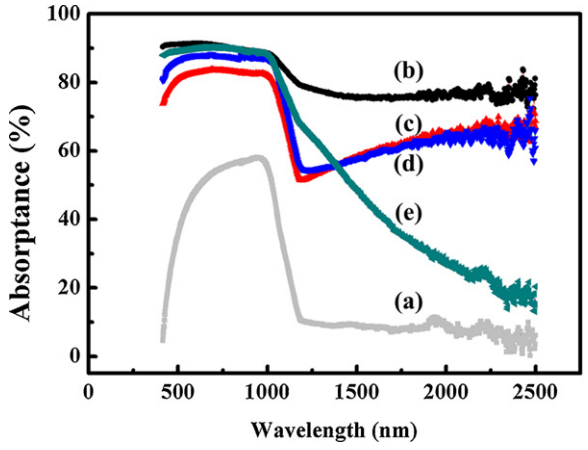

Fig. 5. Dependence of optical absorptance on wavelength of the irradiated silicon with different post-treatments. (a) Flat silicon; (b) Te coated silicon, no annealing; (c) Te coated silicon, after annealing at a temperature of 775 K for 45 min in ambient air; (d) Te coated silicon, etching with 10% HF for 10 min; (e) uncoated silicon, no annealing.

Additionally, we can also see from Fig. 5 (curve (d)) that the near-infrared absorptance of the black silicon keeps nearly invariant after the removing of the incorporated O via the selectively etching with HF. This indicates that the incorporated O contributes little to the enhancement of the near-infrared absorptance. Two additional observations support what we speculated above is reasonable. Firstly, for the unannealed sample, the content of O is much larger than that of Te coated sample (see Fig. 4(b)), but the near-infrared absorptance of the Te coated sample is higher than that of the uncoated sample (see curves (b) and (e) in Fig. 5). Secondly, for the Te coated sample, the content of O increases after annealing (see Fig. 4(b)), but the near-infrared absorption decreases (see curves (b) and (c) in Fig. 5).

Because of the absorption enhancement of the femtosecond laser induced black silicon in the visible and near-infrared regions, it may find some potential applications in silicon based intermediate band gap solar cells [36] and photodiodes [37]. Related investigations such as photo-current, current–voltage characteristics and responsivity of femtosecond laser microstructured solar cells and photodiodes will be the subject of future research.

4. Conclusions

We fabricated black silicon on Te coated silicon substrate in ambient air. Both Te and O were incorporated into silicon after irradiation. By selective etching with HF, the incorporated O species was effectively removed. The absorptance of the black silicon was enhanced in the visible (reaches 90%) and near-infrared regions (reaches 80%). This is an alternative approach for the femtosecond laser induced black silicon in ambient air.

Acknowledgments

The authors gratefully acknowledge the financial support for this work provided by the National Science Foundation of China under the grant no. 91123028, the National Basic Research Program of China (973 Program) under the grant no. 2012CB921804, and the National Science Foundation of China under the grant nos. 61235003 and 11204236.

References

[1] Y. Liu, T. Lai, H. Li, Y. Wang, Z. Mei, H. Liang, Z. Li, F. Zhang, W. Wang, A.Y. Kuznetsov, X. Du, Small 8 (2012) 1392–1397.
[2] Y.F. Huang, S. Chattopadhyay, Y.J. Jen, C.Y. Peng, T.A. Liu, Y.K. Hsu, C.L. Pan, H.C. Lo, C.H. Hsu, Y.H. Chang, C.S. Lee, K.H. Chen, L.C. Chen, Nature Nanotechnology 2 (2007) 770–774.
[3] C. Lee, S.Y. Bae, S. Mobasser, H. Manohara, Nano Letters 5 (2005) 2438–2442.
[4] L. Sainiemi, V. Jokinen, A. Shah, M. Shpak, S. Aura, P. Suvanto, S. Franssila, Advanced Materials 23 (2011) 122–126.
[5] T.-H. Her, R.J. Finlay, C. Wu, S. Deliwala, E. Mazur, Applied Physics Letters 73 (1998) 1673–1675.
[6] Y. Peng, Y. Wen, D. Zhang, S. Luo, L. Chen, Y. Zhu, Applied Optics 50 (2011) 4765–4768.
[7] V. Zorba, N. Boukos, I. Zergioti, C. Fotakis, Applied Optics 47 (2008) 1846–1850.
[8] S. Zhang, Y. Li, G. Feng, B. Zhu, S. Xiao, L. Zhou, L. Zhao, Optics Express 19 (2011) 20462–20467.
[9] M. Sher, M.T. Winkler, E. Mazur, Materials Research Society Bulletin 36 (2011) 439–445.
[10] B.K. Nayak, V.V. Iyengar, M.C. Gupta, Progress in Photovoltaics: Research and Applications 19 (2011) 631–639.
[11] L.Q. Zhu, J. Gong, J. Huang, P. She, M.L. Zeng, L. Li, M.Z. Dai, Q. Wan, Solar Energy Materials and Solar Cells 95 (2011) 3347–3351.
[12] V.V. Iyengar, B.K. Nayak, K.L. More, H.M. Meyer III, M.D. Biegalski, J.V. Li, M.C. Gupta, Solar Energy Materials and Solar Cells 95 (2011) 2745–2751.
[13] Z. Huang, J.E. Carey, M. Liu, X. Guo, E. Mazur, J.C. Campbell, Applied Physics Letters 89 (2006) (033506 (3pp)).
[14] P. Hoyer, M. Theuer, R. Beigang, E.-B. Kley, Applied Physics Letters 93 (2008) (091106 (3pp)).
[15] V. Zorba, E. Stratakis, M. Barberoglou, E. Spanakis, P. Tzanetakis, S.H. Anastasiadis, C. Fotakis, Advanced Materials 20 (2008) 4049–4054.
[16] T. Baldacchini, J.E. Carey, M. Zhou, E. Mazur, Langmuir 22 (2006) 4917–4919.
[17] M.A. Sheehy, L. Winston, J.E. Carey, C.M. Friend, E. Mazur, Chemistry of Materials 17 (2005) 3582–3586.
[18] B.R. Tull, J.E. Carey, E. Mazur, J.P. McDonald, S.M. Yalisove, Materials Research Society Bulletin 31 (2006) 627–633.
[19] M.J. Smith, M. Winkler, M.-J. Sher, Y.-T. Lin, E. Mazur, S. Gradečak, Applied Physics A105 (2011) 795–800.
[20] G. Feng, Y. Li, Y. Wang, P. Li, J. Zhu, L. Zhao, Optics Letters 37 (2012) 299–301.
[21] M. Halbwax, T. Sarnet, P. Delaporte, M. Sentis, H. Etienne, F. Torregrosa, V. Vervisch, I. Perichaud, S. Martinuzzi, Thin Solid Films 516 (2008) 6791–6795.
[22] A.V. Kabashin, P. Delaporte, A. Pereira, D. Grojo, R. Torres, T. Sarnet, M. Sentis, Nanoscale Research Letters 5 (2010) 454–463.
[23] T.G. Kim, J.M. Warrender, M.J. Aziz, Applied Physics Letters 88 (2006) (241902 (3pp)).
[24] M.A. Sheehy, B.R. Tull, C.M. Friend, E. Mazur, Materials Science and Engineering B137 (2007) 289–294.
[25] S.H. Pan, D. Recht, S. Charnvanichborikarn, J.S. Williams, M.J. Aziz, Applied Physics Letters 98 (2011) (121913 (3pp)).
[26] R. Younkin, J.E. Carey, E. Mazur, J.A. Levinson, C.M. Friend, Journal of Applied Physics 93 (2003) 5.
[27] D. Mills, K.W. Kolasinski, Nanotechnology 17 (2006) 2741–2744.
[28] K.W. Kolasinski, Current Opinion in Solid State and Materials Science 11 (2007) 76–85.
[29] B.K. Nayak, M.C. Gupta, K.W. Kolasinski, Nanotechnology 18 (2007) (195302 (4pp)).
[30] Y. Izawa, Y. Izawa, Y. Setsuhara, M. Hashida, M. Fujita, R. Sasaki, H. Nagai, M. Yoshida, Applied Physics Letters 90 (2007) (044107 (2pp)).
[31] T. Kudrius, G. Slekys, S. Juodkazis, Journal of Physics D: Applied Physics 43 (2010) (145501 (5pp)).
[32] Y. Ma, H. Shi, J. Si, T. Chen, F. Yan, F. Chen, X. Hou, Optics Communication 285 (2012) 140–142.
[33] Y. Ma, H. Shi, J. Si, H. Ren, T. Chen, F. Chen, X. Hou, Journal of Applied Physics 111 (2012) (093102 (4pp)).
[34] A. Somashekhar, S. O'Brien, Journal of the Electrochemical Society 143 (1996) 2885–2891.
[35] A.A. Pande, D.S.L. Mui, D.W. Hess, IEEE Transactions on Semiconductor Manufacturing 24 (2011) 104–116.
[36] A. Luque, A. Martí, C. Stanley, Nature Photonics 6 (2012) 146–152.
[37] J.E. Carey, C.H. Crouch, M. Shen, E. Mazur, Optics Letters 30 (2005) 1773–1775.